Interner Bericht

DESY-H/18

September 1969

FINAL PARAMETERS AND STATUS OF DESY DOUBLE STORAGE RING

von

K. Steffen

150 - 170

DESY - H/18 Hamburg, den 18. September 1969

FINAL PARAMETERS AND STATUS OF DESY DOUBLE STORAGE RING

von

K. Steffen

(Invited paper at the 7th International Accelerator Conference, Yerevan, 27th August - 2nd September 1969)

Since the fall of 1967, when the proposal of the DESY 3 GeV double storage ring was submitted, the continuous review and further development of the project has lead us to improve many features in detail but has, however, convinced us that the basic concept and ring geometry should be maintained.

The most fundamental question raised by these investigations and especially by the new double storage ring schemes proposed at SLAC and Orsay was that of crossing geometry and luminosity as limited by the incoherent space charge effect. Applying the schemes of

- small angle vertical crossing, or
- large angle horizontal crossing, or
- space charge compensated 4-bunch collision, respectively

to the DESY-rings, we obtained the luminosity curves shown in Fig. 1. The solid curves No. 1 and 2 refer to small angle vertical crossing with two different values β_x of the horizontal amplitude function at interaction point and the same value β_z = 10 cm. The lower curve holds for β_x = 10 cm, where the full ring acceptances ε_x = 8mradcm and ε_z = 0,8mradcm are available, as needed for injection. After injection, β_x can be reduced to 2,5 cm, which reduces the horizontal acceptance to 2mradcm. Applying this reduction to the extent compatible with natural beam width, the upper luminosity curve is obtained. The crossing angle is chosen just large enough to vertically separate the beams and varies between 12mrad and 28mrad, depending on energy. For high energies, the bunch population number is varied too, assuming that only every 2nd, 4th, 8th or 16th bucket, respectively, is filled. The dotted curve No. 3 is obtained for horizontal crossing with $\beta_x = \beta_z$ = 10 cm at a fixed crossing angle of 200mrad, the population number being varied as before at high energies. The curves No. 1, 2 and 3 are calculated for an rf frequency of 500 MHz but are insensitive to changing the harmonic number. Curve No. 4 shows the luminosity for the space charge compensated scheme with an rf frequency of 5 MHz and only two oppositely circulating bunches in each beam (β_x, β_z > 30 cm).

Since the luminosity for all schemes is of the same order, we have decided to stay with the small angle vertical crossing, thus avoiding a substantial increase in construction time and cost of the buildings.

In distinction to our 1967 proposal, we have now eliminated the high voltage electrostatic separators, at least for the initial stage of construction, by slightly increasing the crossing angle such that the beams can be separated by inserting a current sheet septum between them. The main vertical beam displacement is then achieved by two vertically bending double magnets as described in the original proposal. The vertical dispersion introduced by these magnets allows to vary the natural beam height by varying the optical matching of the long straight sections. A side view of the crossing geometry with vertical beam envelopes is shown in Fig. 2. Before reaching the septum, the beams pass through two common large aperture quadrupoles, which are shown in Fig. 3. The apertures available for the upper and lower beam in the first and second quadrupole, respectively, are indicated by ellipses. The quadrupole next to the interaction point is horizontally focusing. With $\beta_x = \beta_z = 10$ cm at interaction point, the maximum values of the amplitude function are 90 m and 700 m, respectively. The expected closed orbit deviation generated by a statistical misalignment of 0,1 mm in these 8 quadrupoles is smaller than 4 cm and 20 cm, respectively, and will be controlled by beam steering.

The main ring geometry has not been changed (Fig. 4). Each quadrant consists of 3 mechanically identical magnet periods surrounded by a short straight section for injection and the long straight section holding the interaction region, the vertical beam separation and the radiofrequency system. The two short straights not needed for injection may be used for controlling the damping distribution by displacing the beam in a quadrupole channel. Fig. 5 shows the horizontal and vertical beam envelopes in one quadrant between interaction point (left) and injection

point (right). The Q-values are 10,1 and 4,1 for the horizontal and vertical motion, respectively; they can be varied by about ± 1. The horizontal dispersion is matched to be zero in the long straights while, for minimum natural beam height, the vertical dispersion can be matched to be zero in the ring parts.

Fig. 6 gives the cross section of the bending magnets, which are curved and made of solid low carbon steel. The tracking of solid magnets has been tested at DESY and was found satisfactory. All magnets have been changed to allow a maximum beam energy of 4.5 GeV; correspondingly, the vertical displacement between beams was raised to 80 cm. The stainless steel vacuum chamber (Fig. 7) has outside ribs for reinforcement and can be baked in place. Ion getter pumps are located between the upper and lower chamber.

The double quadrupoles (Fig. 8) will be manufactured with high intrinsic and relative accuracy using precision assembly jigs. Correction coils around and between the poles allow to superimpose corrected horizontal and vertical dipole fields for beam steering. The aperture has been increased to hold a circular vacuum chamber of 14,4 cm inner diameter which - with the exception of bending magnets and interaction regions - continues as a smooth pipe around the ring.

A magnet period is shown in Fig. 9. The absorbers for synchrotron radiation are located in boxes extending the vacuum chambers beyond the ends of the magnets; they will probably be large, water cooled copper cylinders with a V-groove.

The 500 MHz radiofrequency system has 3 klystron transmitters of 250 kW cw for each beam. Each transmitter feeds 4 cylindrical single cavities through a waveguide system incorporating an isolator and magic tees for decoupling of cavities.

An axial view of the cavity is given in Fig. 10, showing the input loop coupler, a tuning plunger and a measuring loop. The Q-value is 40 000 and the shunt impedance 3 MΩ. In beam loaded operation, the cavity is kept tuned on resonance by

controlling the plunger. Since the available frequency shift is limited to about 2 MHz, the synchronous phase angle must be small at low energies and, in addition, the total shunt impedance must be reduced by detuning part of the cavities.

The site layout is shown in Fig. 11. Injection is done at about 1.5 GeV from the synchrotron or, mainly for beam tests, directly from the new 400 MeV electron-positron linac. Typical injection times from the synchrotron are 2.5 sec/Ampere for electrons and 2.5 min/Ampere for positrons.

The floor of the high bay connecting the two interaction points is 1.7 meters below beam level. A hole with an area of 8 x 8 m^2 and a depth of 4,5 m below beam level is available at one side for varying experimental setups while, at the other side, a much larger hole of same depth is planned for a large retractable magnetic detector. Figure 12 shows an artist's view of the buildings.

Construction funds for the project are available starting this year. The orders for rf transmitters and main ring magnets will be placed within the near future, building construction will start next spring, and the storage ring is expected to be completed in 1973.

August 1969

Parameters of DESY Double Storage Ring

1. Magnet lattice

Number of magnet periods		2 • 12
Length of magnet period		13,2 m
Mean radius (without long straights)		26,74 m
Radius of curvature in magnets		12,19 m
Deflecting field at 3 BeV		8,1 KГ
Field gradient in qadrupoles		
at Q_x = 10,1 and Q_z = 4,1 between 0,4 KГ/cm and 0,86KГ/cm		
Amplitude function in bending magnets		
	Maximum	11,5 m
horizontal		
	Minimum	1,4 m
	Maximum	13,5 m
vertical		
	Minimum	11,3 m
Maximum amplitude function in the ring		
horizontal		87,5 m.
vertical		706 m
Amplitude function at interaction point		
horizontal		0,1 m
vertical		0,1 m
Dispersion in bending magnets		
	Maximum	2,2 m
horizontal		
	Minimum	0 m
	Maximum	0 m
vertical		
	Minimum	0 m
Momentum compaction factor		$1,8 \cdot 10^{-2}$
Crossing angle $\delta = 2\phi$ vertical between 12 and 28mrad		
Number of long straight sections		2
Length of long straight section		60 m
Length of principal orbit		288 m

Mean radius including long straights	$\overline{R}$ = 45,84 m
Frequency of revolution	f_o = 1,0410 MHz
Iron weight:	
Bending magnets	550 t
Quadrupoles	240 t
Copper weight:	
Bending magnets	40 t
Quadrupoles	28 t
Magnet Power at 3 BeV	5,6 MWatt

B. Rf system

Harmonic number	480
Frequency	499,67 MHz
Number of klystrons	2 • 3
Number of cavities	2 • 12
Maximum rf power	2 • 0,75 MWatt cw
Peak rf voltage per ring at 3 BeV and 16° synchronous phase angle	3,5 MV
Rf beam power at 3 BeV and 16° synchronous phase angle	2 • 0,55 MWatt cw

Vacuum system

Ion getter pumps	
Number of 120 l pump units	96
Number of 240 l pumps	96
Number of 450 l pumps	64
Number of 1000 l pumps	12
Total pumping speed for N_2 at $5 \cdot 10^{-9}$ Torr	$5,6 \cdot 10^4$ l sec^{-1}
Number of ion sputter pumps (open)	48
Number of cryopumps in interaction regions	4
Turbomolecular pumps	
Number of 200 l - 300 l pumps	48
Average partial pressures in vacuum system	
Without beam N_2, CO	$1 \cdot 10^{-9}$ Torr
H_2	$< 1 \cdot 10^{-9}$ Torr

With beam (1A at 3 BeV)	N_2,CO	$6,5 \cdot 10^{-9}$ Torr
	H_2	$4,5 \cdot 10^{-9}$ Torr

Injection system

Injection efficiency	50 %
Acceptance	0,5 mrad cm
Energy spread	± 0,5 %
Injection time at about 1,5 BeV	
Electrons	2,6 sec/A
Positrons	150 sec/A

Beam parameters at 1.5 BeV and 3 BeV

	1,5 BeV	3 BeV
Design luminosity	$9 \cdot 10^{32}$ cm^{-2} sec^{-1}	$1 \cdot 10^{32}$ cm^{-2} sec^{-1}
Beam current	2 x 6 A	2 x 0,9 A
Number of particles	2 x $3,7 \cdot 10^{13}$	2 x $5,6 \cdot 10^{12}$
Bunch population number	1	4
Half crossing angle at interaction point	14 mrad	6 mrad
Synchronous phase	1^o	16^o
Peak rf voltage per ring	3,4 MV	3,5 MV
Radiation loss	2 x 228 kW	2 x 550 kW
Damping times		
Betatron oscillation	80 msec	10 msec
Synchrotron oscillation	37 msec	4,6 msec
Energy spread	0,54 MeV	2,1 MeV
Bunch length ($2\sigma_L$)	1,3 cm	3,8 cm
Beam life due to quantum fluctuations	> 10^{30} h	$2,6 \cdot 10^6$ h
Beam life due to brems-strahlung on residual gas	3,9 h	9 h
Beam life due to brems-strahlung on the other beam at design luminosity	86 h	100 h
"natural" beam emittance		
horizontal	$1 \cdot 10^{-2}$ mrad cm	$4,0 \cdot 10^{-2}$ mrad cm
vertical	$4,5 \cdot 10^{-5}$ mradcm	$9,3 \cdot 10^{-6}$ mrad cm

	1,5 BeV	3 BeV
"natural" beam dinensions at interaction point		
half beam width (σ_x)	100 µm	200 µm
half beam height (σ_z)	6,7 µm	3,1 µm
Beam emittance required for design luminosity		
horizontal	$3,2 \cdot 10^{-2}$ mradcm	$4,0 \cdot 10^{-2}$ mradcm
vertical	$1,2 \cdot 10^{-2}$ mradcm	$1,0 \cdot 10^{-4}$ mradcm
Beam dimensions required for design luminosity at interaction point		
half beam width (σ_x)	180 µm	200 µm
half beam height (σ_z)	110 µm	> 10 µm

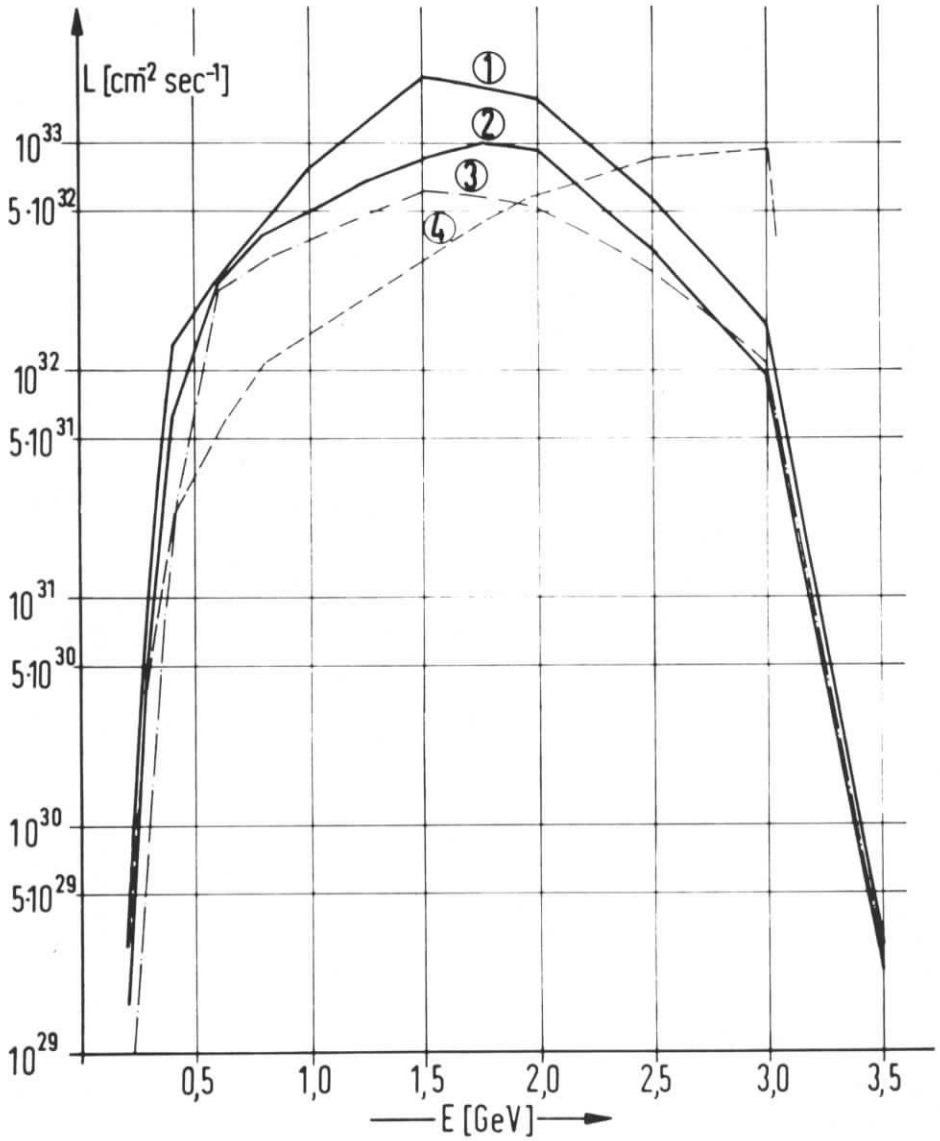

① vertical crossing ; 12 mrad $\leq \delta \leq$ 28 mrad; $\beta_x \geq 0.025$ m ; $\beta_z \geq 0.1$ m

② —"— 12 mrad $\leq \delta \leq$ 28 mrad; $\beta_x = 0.1$ m ; $\beta_z = 0.1$ m

③ horizontal crossing; $\delta = 200$ mrad; $\beta_x \geq 0.025$ m ; $\beta_z = 0.1$ m

④ space charge compensated one bunch $\delta = 0$ mrad ; $\beta_x \geq 1.0$ m ; $\beta_z = 0.3$ m

Luminosity vs Energy

Fig. 1

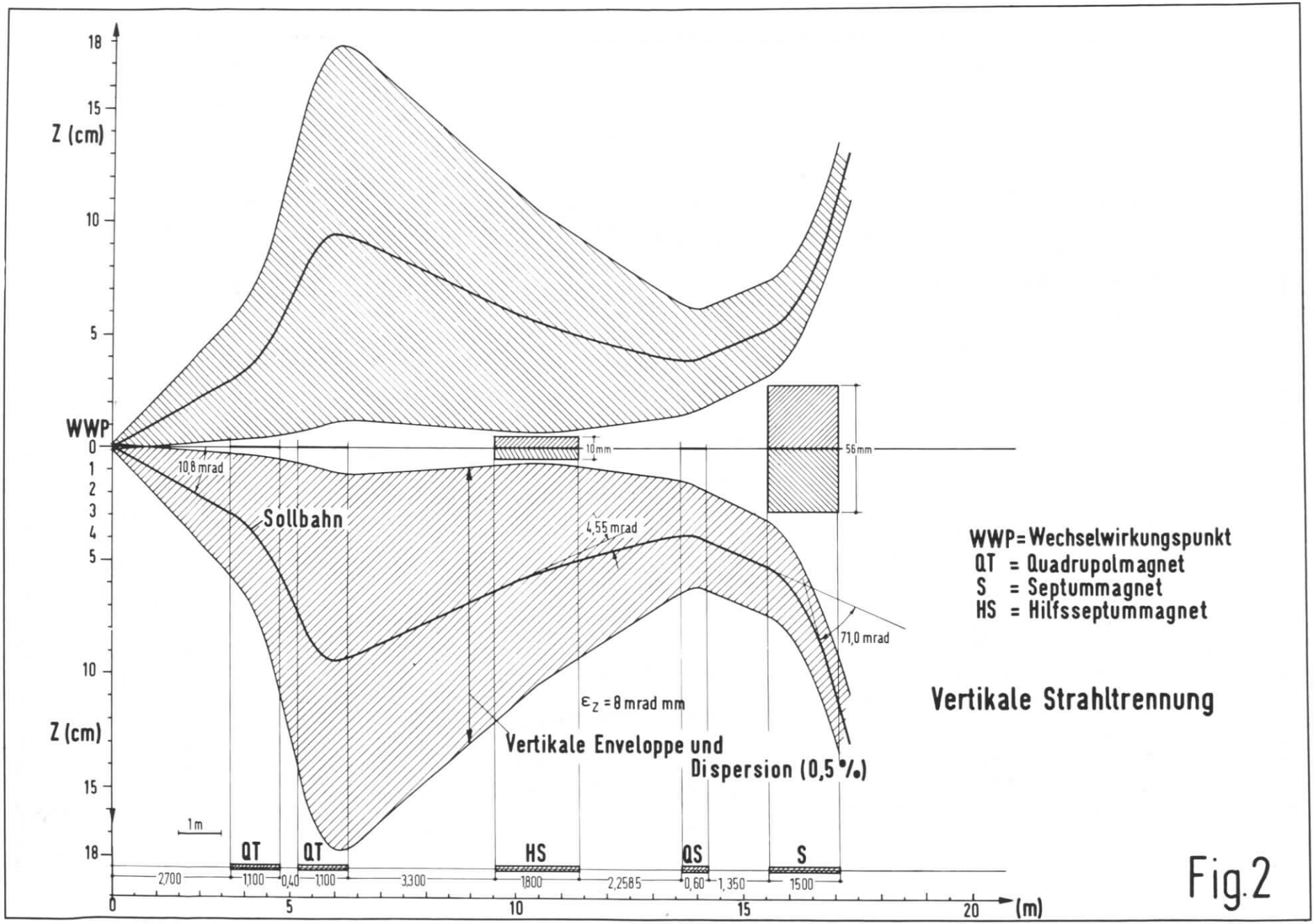
Z (cm)
WWP
10,8 mrad
Sollbahn
4,55 mrad
71,0 mrad
10mm
56mm
ε_z = 8 mrad mm
Vertikale Enveloppe und
Dispersion (0,5 %)
WWP= Wechselwirkungspunkt
QT = Quadrupolmagnet
S = Septummagnet
HS = Hilfsseptummagnet
Vertikale Strahltrennung
1m
QT
QT
HS
QS
S
2700
1100
400
1100
3300
1800
2258,5
600
1350
1500
(m)

Fig.2

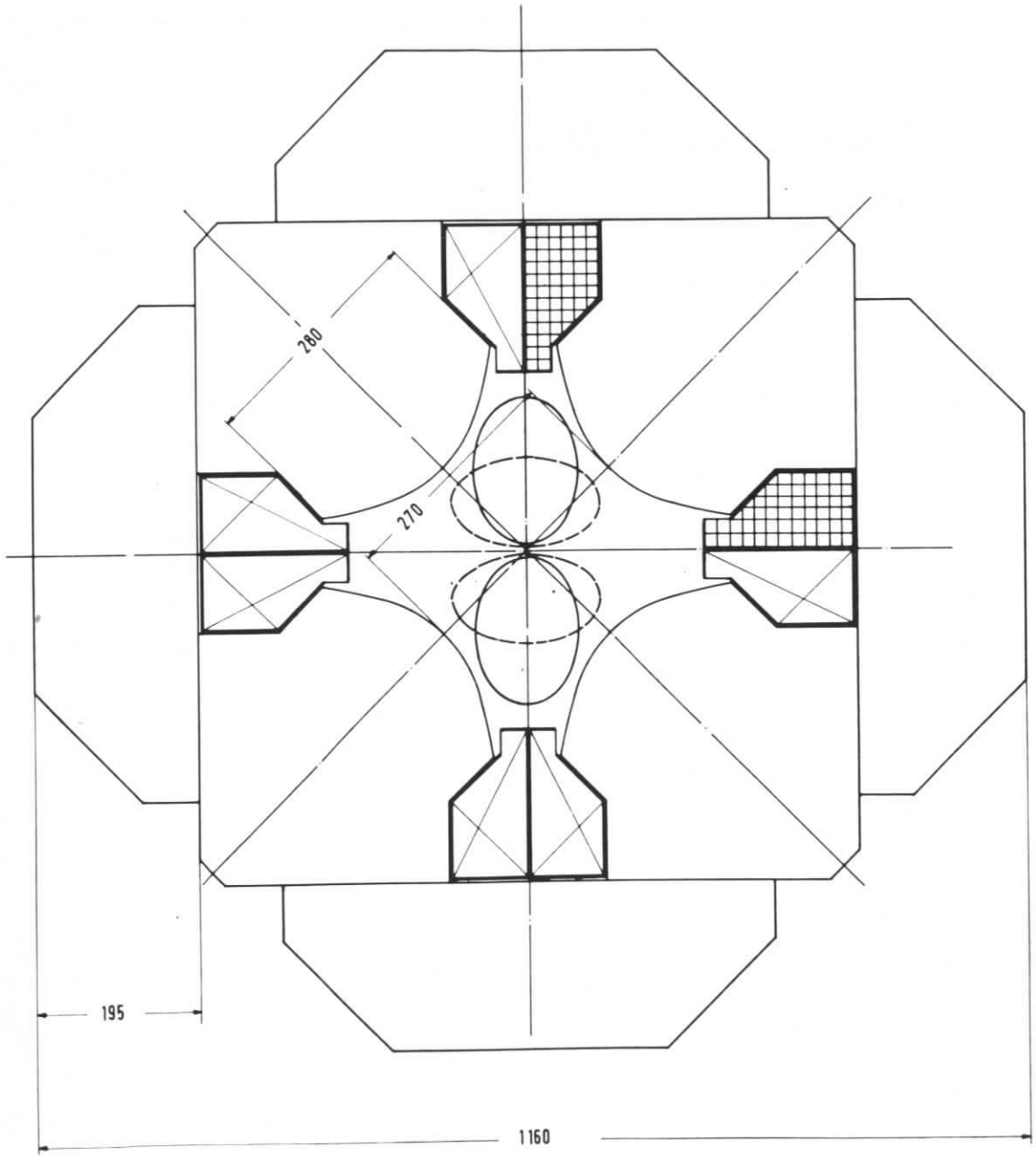

Quadrupol Typ QT

Technische Daten (3 GeV)

Feldgradient	0,7	KT/cm
magnetische Länge	1100	mm
Stromstärke	940	A
Spannung	100	V
Leistung	100	KW
Gewicht	8	t

Fig.3

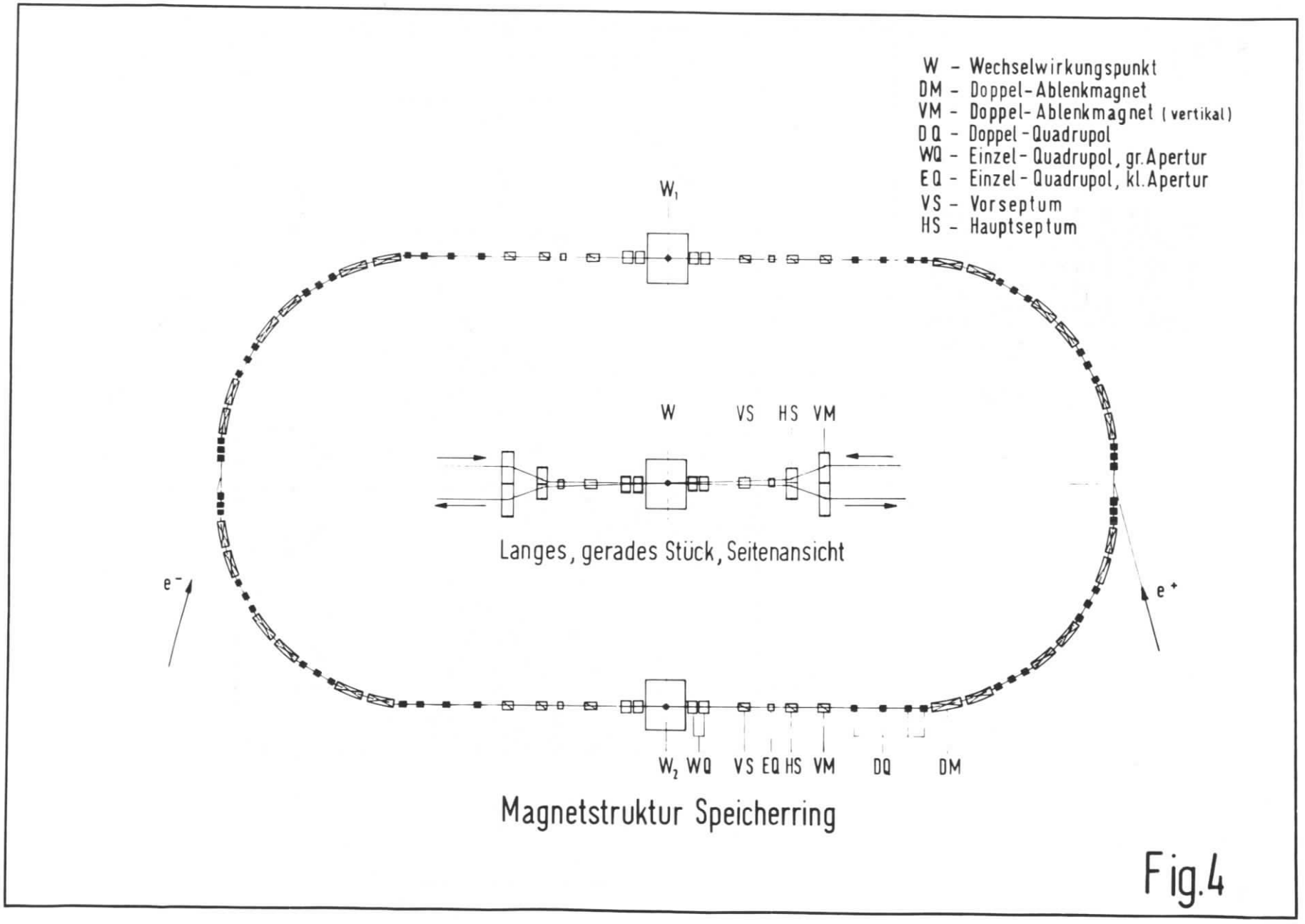
W - Wechselwirkungspunkt
DM - Doppel-Ablenkmagnet
VM - Doppel-Ablenkmagnet (vertikal)
DQ - Doppel-Quadrupol
WQ - Einzel-Quadrupol, gr. Apertur
EQ - Einzel-Quadrupol, kl. Apertur
VS - Vorseptum
HS - Hauptseptum
W1
W VS HS VM
Langes, gerades Stück, Seitenansicht
e⁻
e⁺
W2 WQ VS EQ HS VM DQ DM
Magnetstruktur Speicherring
Fig.4

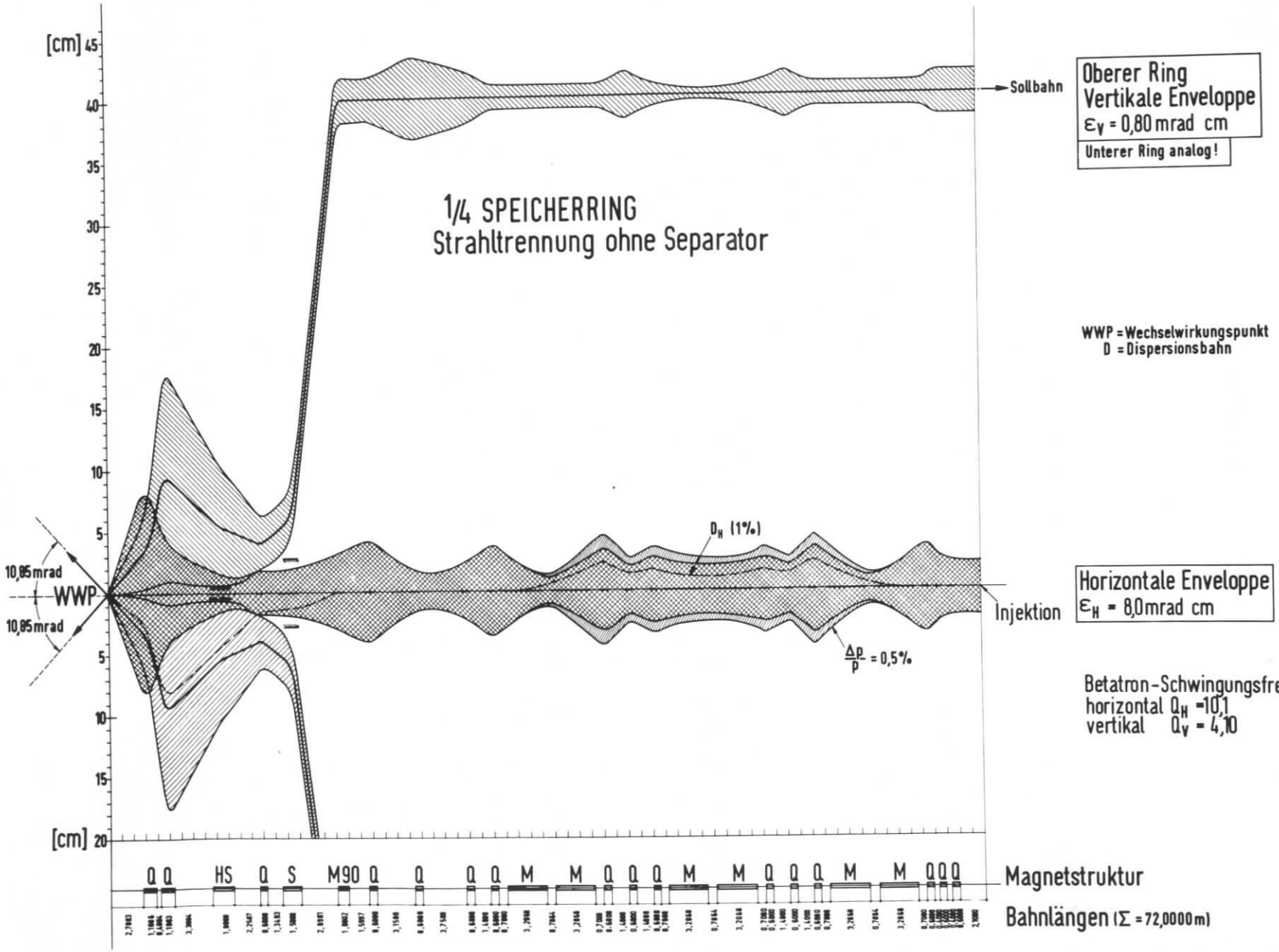
[cm]
45
40
35
30
25
20
15
10
5
5
10
15
20
[cm]
1/4 SPEICHERRING
Strahltrennung ohne Separator
Sollbahn
Oberer Ring
Vertikale Enveloppe
ε_V = 0,80 mrad cm
Unterer Ring analog!
WWP = Wechselwirkungspunkt
D = Dispersionsbahn
D_H (1%)
10,85 mrad
WWP
10,85 mrad
Injektion
Horizontale Enveloppe
ε_H = 8,0 mrad cm
$\frac{\Delta p}{p}$ = 0,5%
Betatron-Schwingungsfrequenz:
horizontal Q_H = 10,1
vertikal Q_V = 4,10
Q Q HS Q S M90 Q Q Q Q M M Q Q Q M M Q Q Q M M Q Q Q
Magnetstruktur
Bahnlängen (Σ = 72,0000 m)

Fig.5

Doppel-Ablenkmagnet

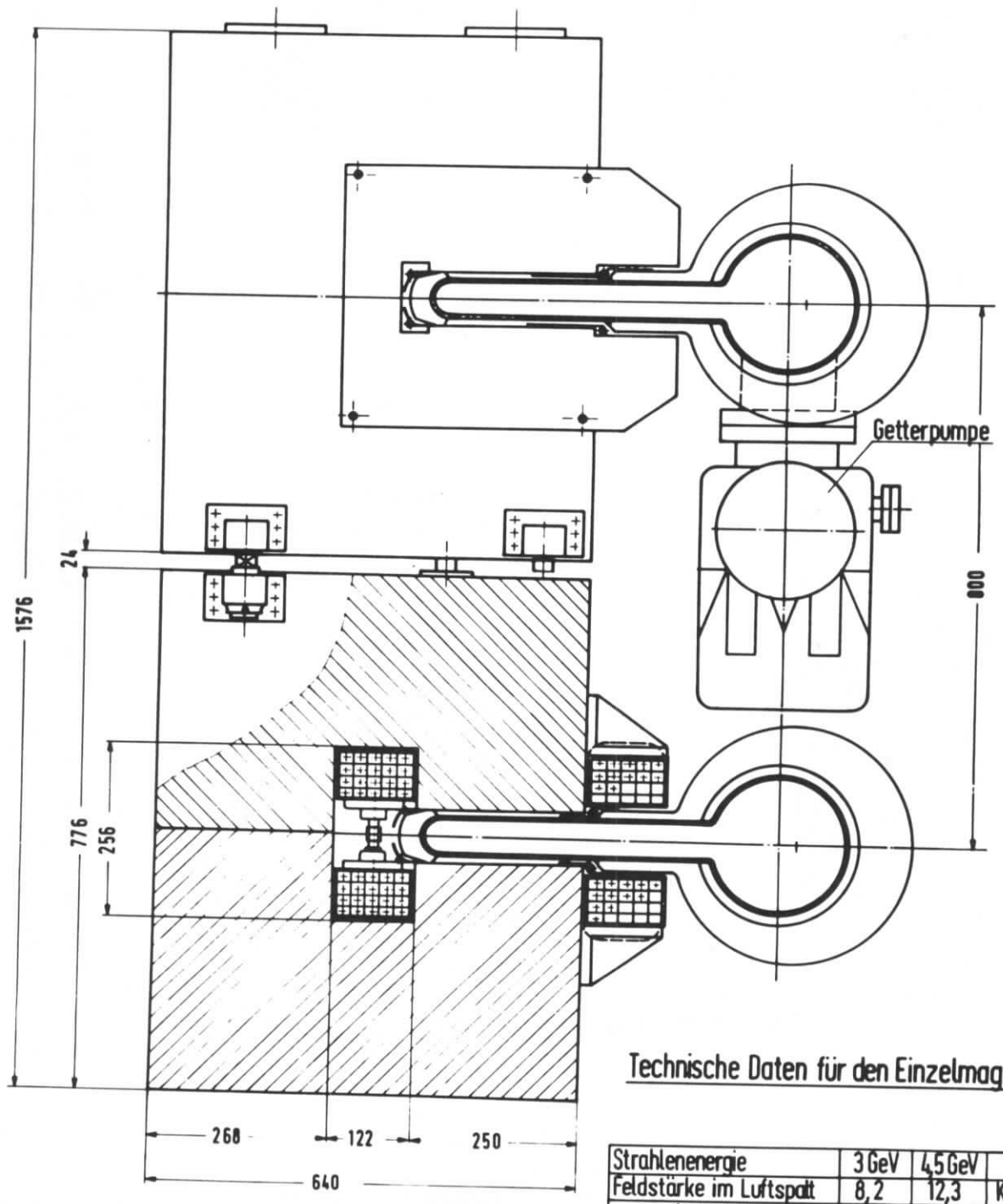

Technische Daten für den Einzelmagneten

Strahlenenergie	3 GeV	4,5 GeV	
Feldstärke im Luftspalt	8,2	12,3	KT
magnetische Länge	3190	3190	mm
Stromstärke	1280	2000	A
Spannung	23,5	36,6	V
Leistung	30	73	KW
Gewicht (o. Kammer)		11,5	t

Fig.6

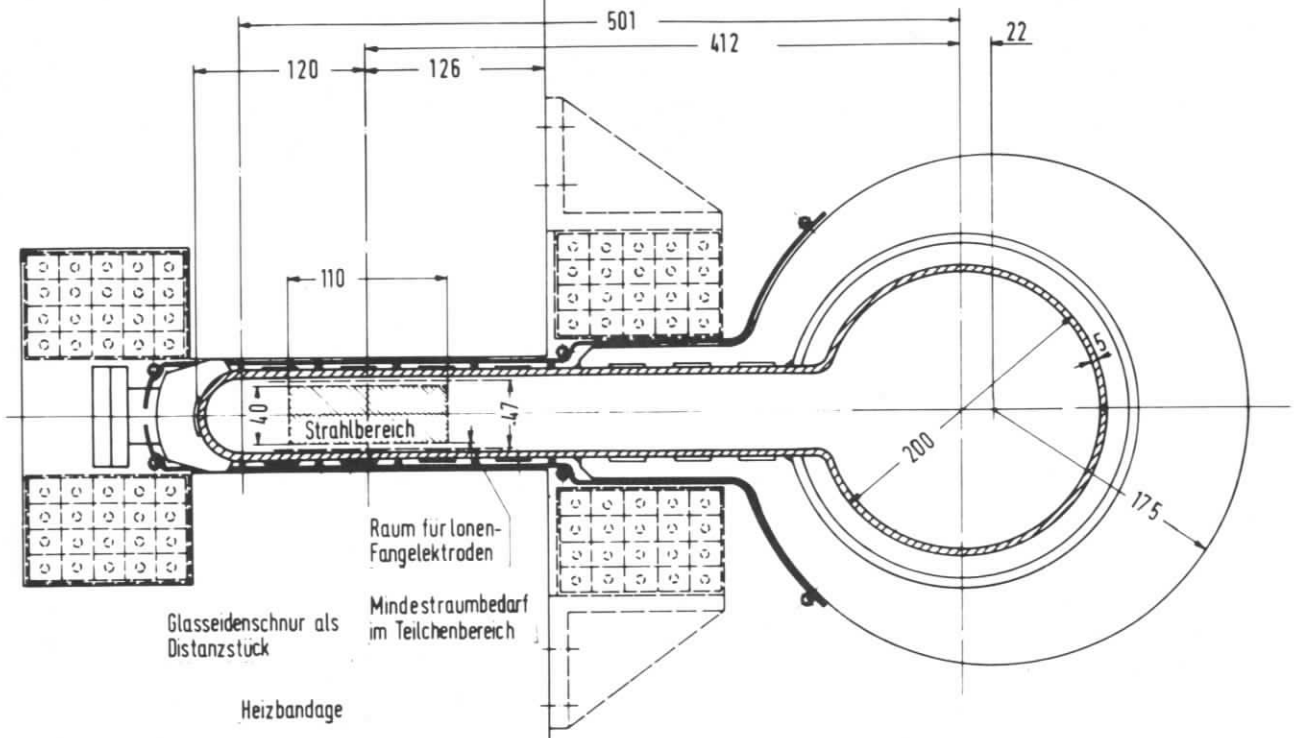

DESY		8.8.69	Fruttke	Gruppe: B
Maßstab	Querschnitt mit schemat. Sandwich Führungsmagnetkammer-Speicherring			Zeichn. No. Blatt No. Ersatz für: Ersetzt durch: x ausf.: ausgef. von: Auftrag No.:

Fig.7

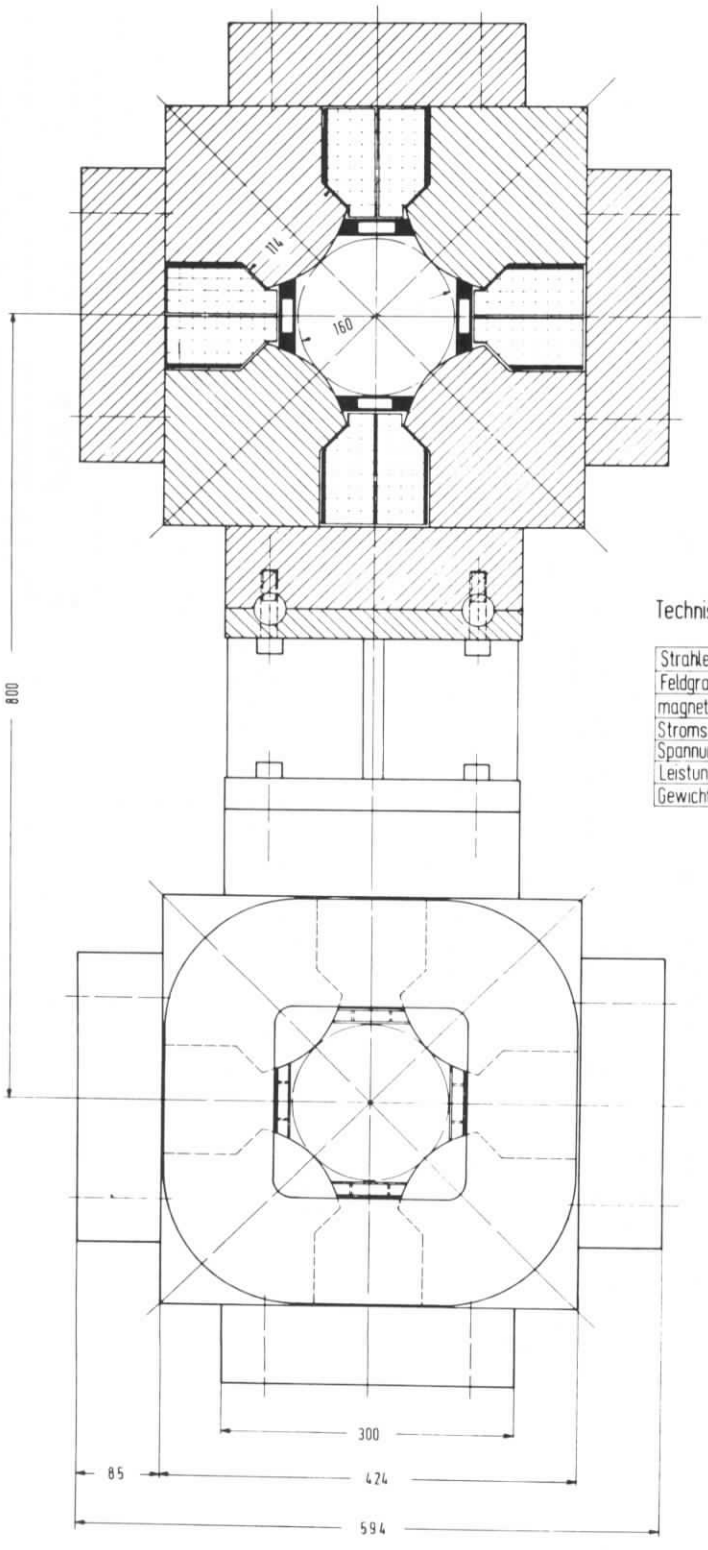

Doppel - Quadrupol

Technische Daten für den Einzelmagneten

Strahlenergie	3 GeV	4,5 GeV	
Feldgradient	0,9	1,35	K T/cm
magnetische Lange	600	600	mm
Stromstarke	740	1110	A
Spannung	38	57	V
Leistung	23	63	K W
Gewicht	2,8		t

Fig.8

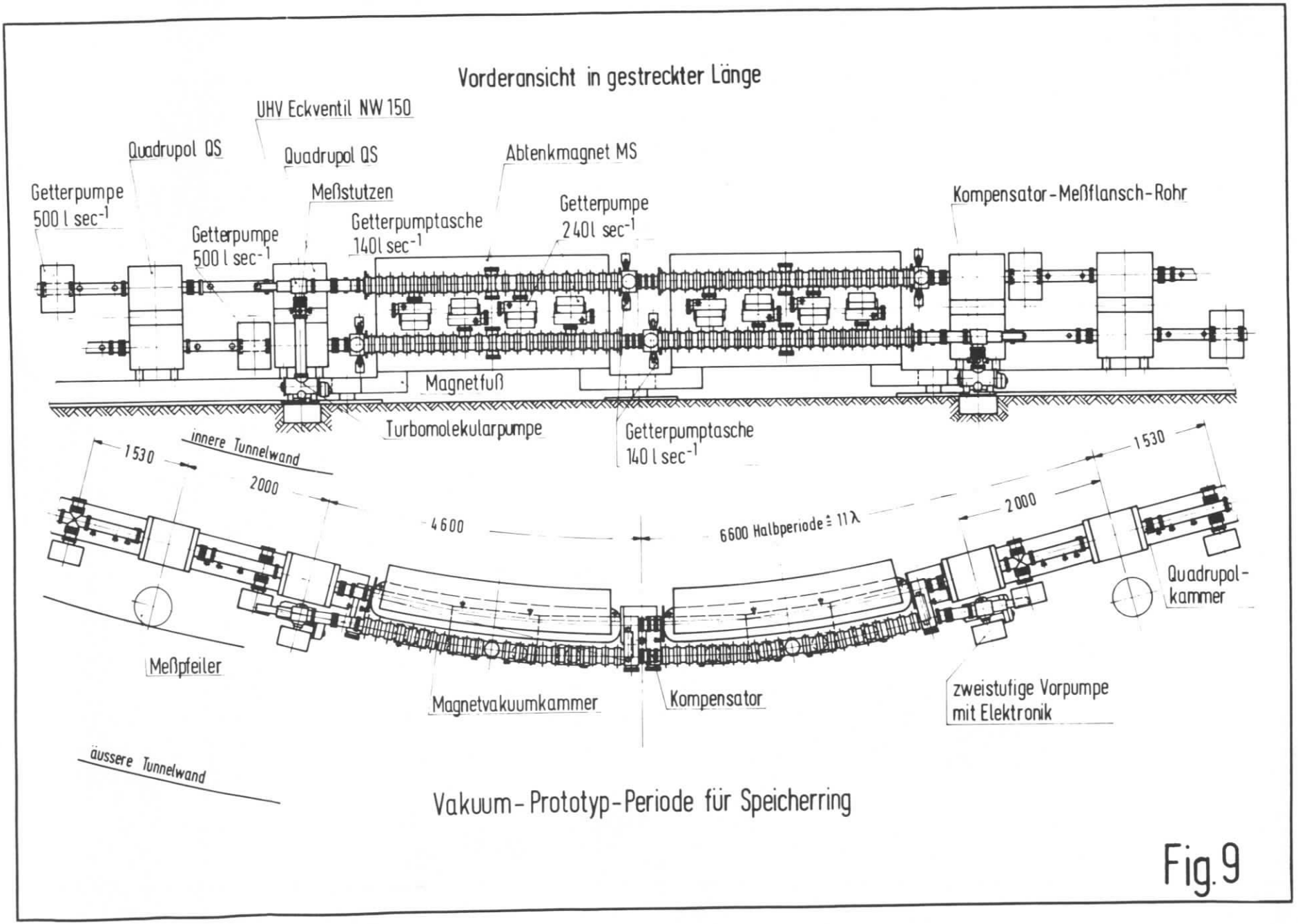
Vorderansicht in gestreckter Länge
UHV Eckventil NW 150
Quadrupol QS
Quadrupol QS
Ablenkmagnet MS
Getterpumpe 500 l sec⁻¹
Meßstutzen
Getterpumpe 500 l sec⁻¹
Getterpumptasche 140l sec⁻¹
Getterpumpe 240l sec⁻¹
Kompensator-Meßflansch-Rohr
Magnetfuß
Turbomolekularpumpe
Getterpumptasche 140 l sec⁻¹
innere Tunnelwand
1530
2000
4600
6600 Halbperiode ≙ 11 λ
2000
1530
Quadrupol-kammer
Meßpfeiler
Magnetvakuumkammer
Kompensator
zweistufige Vorpumpe mit Elektronik
äussere Tunnelwand
Vakuum-Prototyp-Periode für Speicherring
Fig. 9

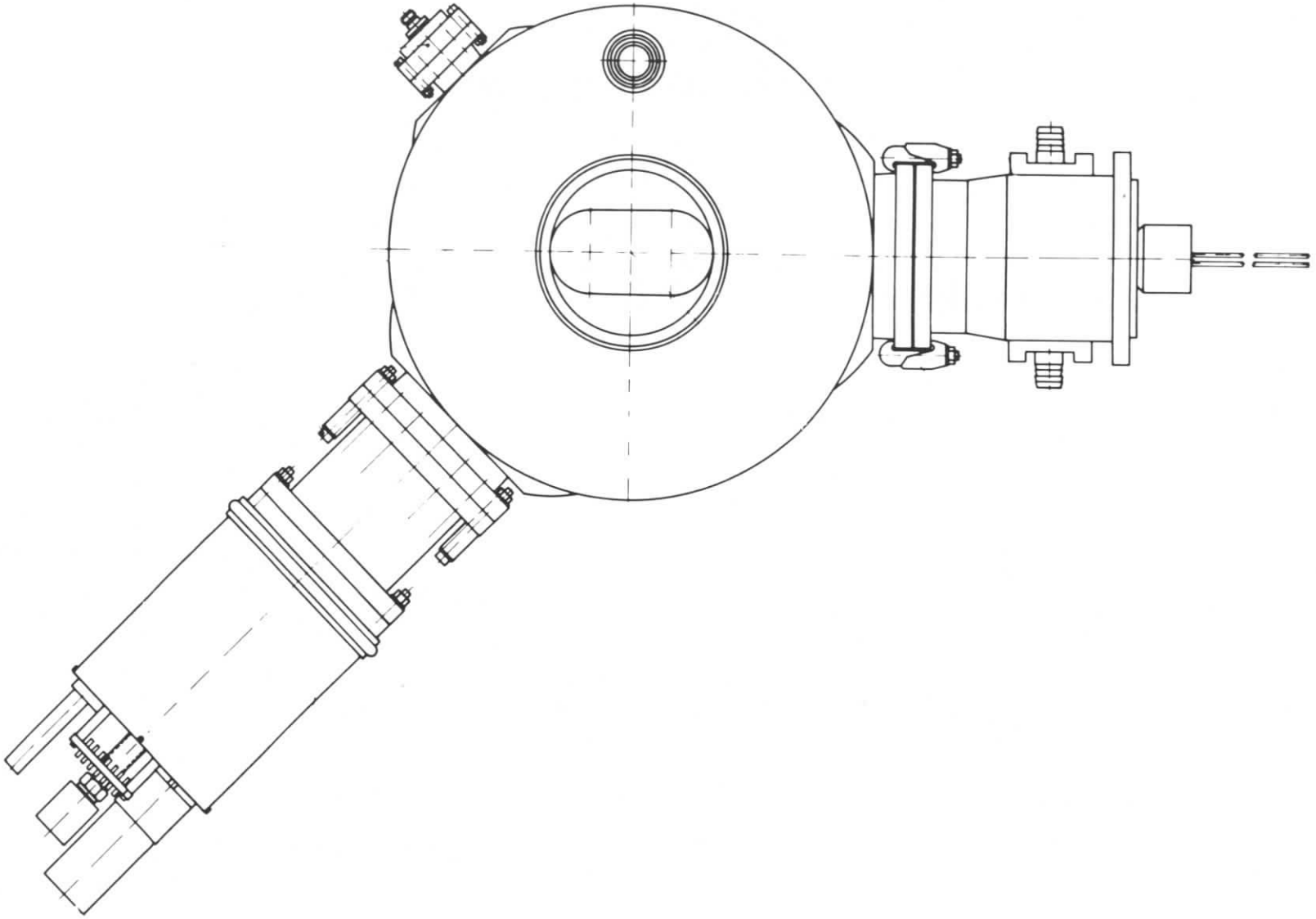

Fig. 10

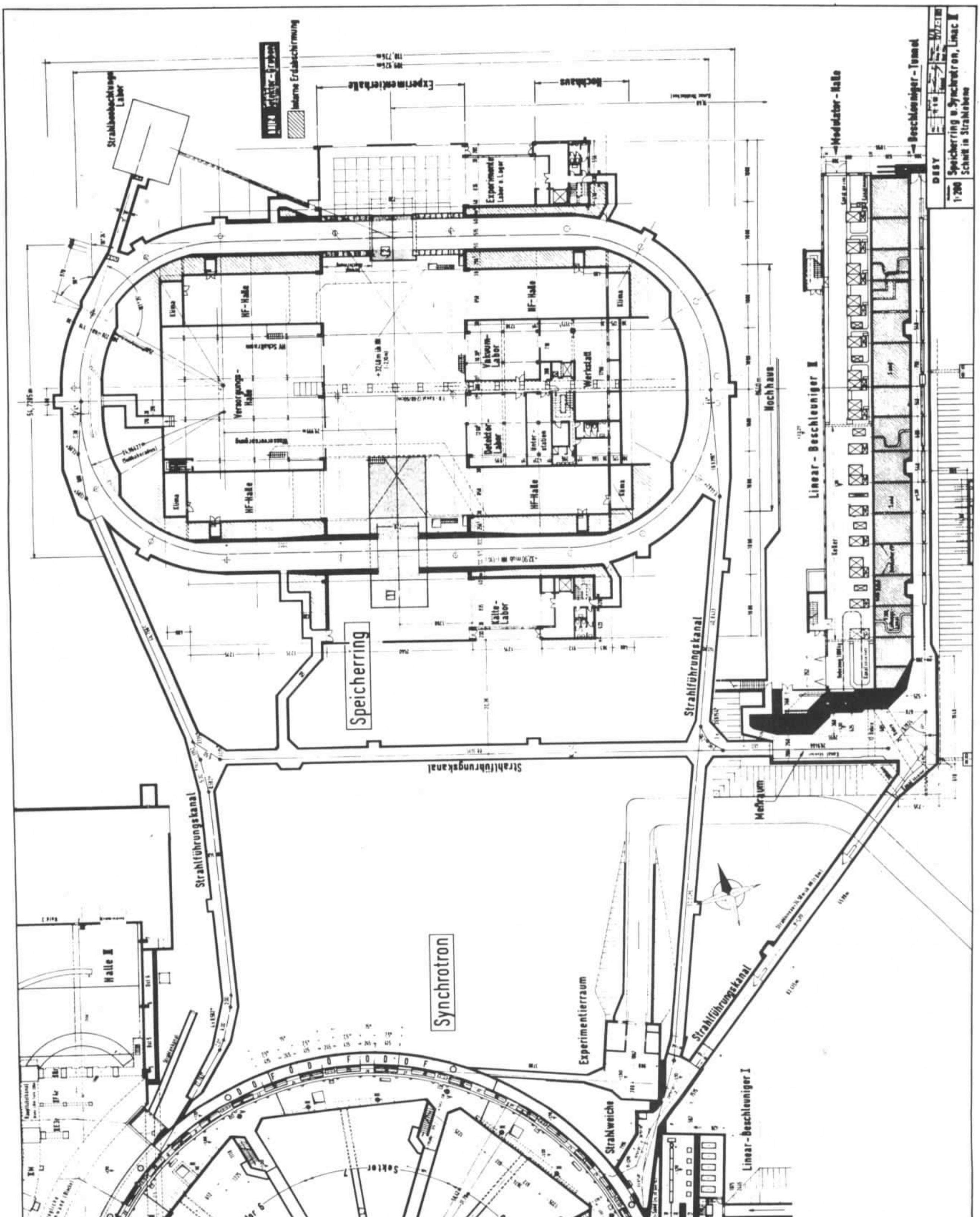
Speicherring
Synchrotron
Strahlführungskanal
Experimentierhalle
Hochhaus
Linear-Beschleuniger II
Linear-Beschleuniger I
Modulator-Halle
Beschleuniger-Tunnel
Meßraum
Experimentierraum
Strahlweiche
Halle II
NF-Halle
Werkstatt
Vakuum-Labor
Kälte-Labor
DESY
1:200
Speicherring u. Synchrotron, Linac II
Schnitt in Strahlebene

Fig.11

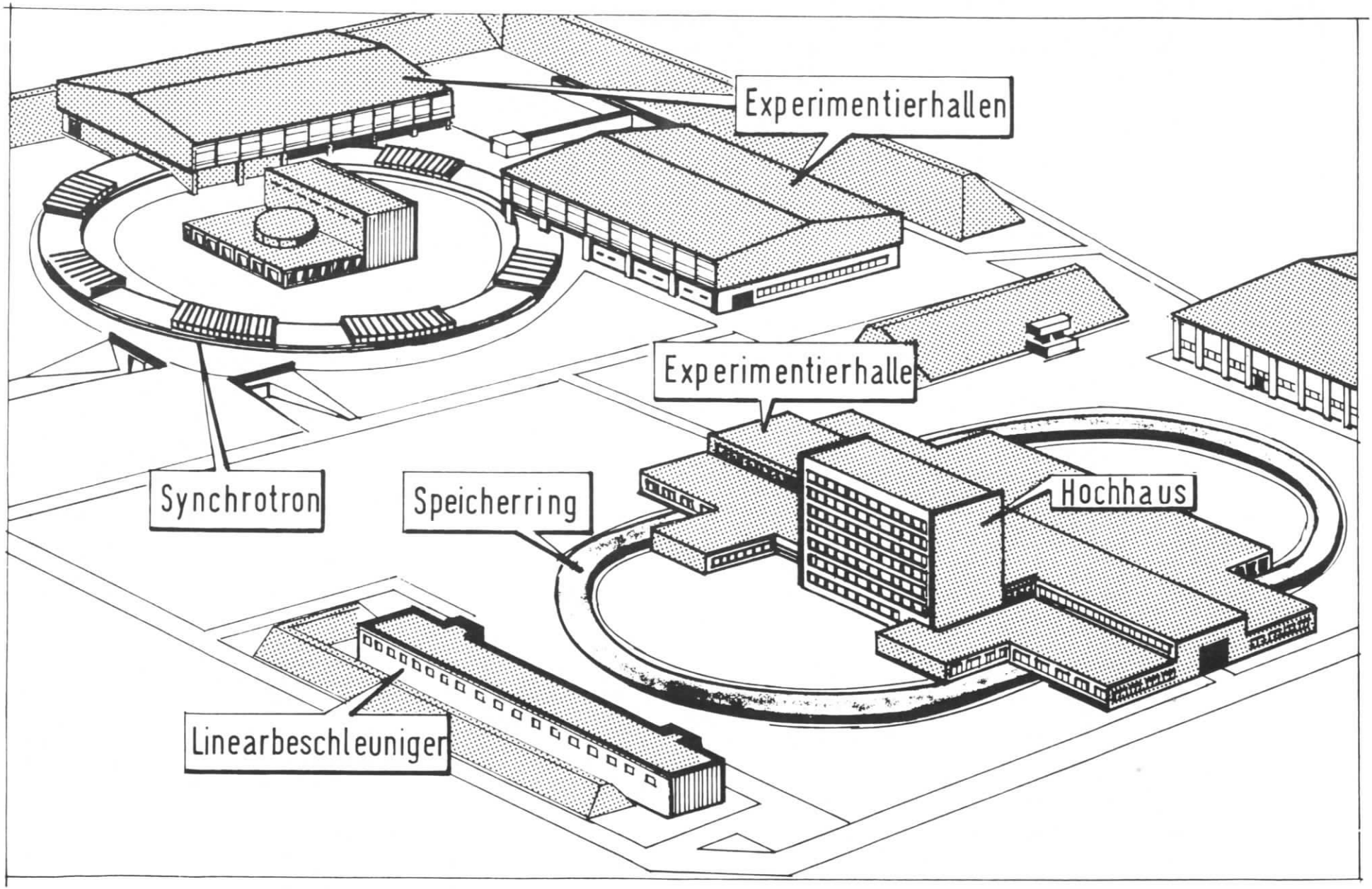
Experimentierhallen
Experimentierhalle
Synchrotron
Speicherring
Hochhaus
Linearbeschleuniger

Fig.12

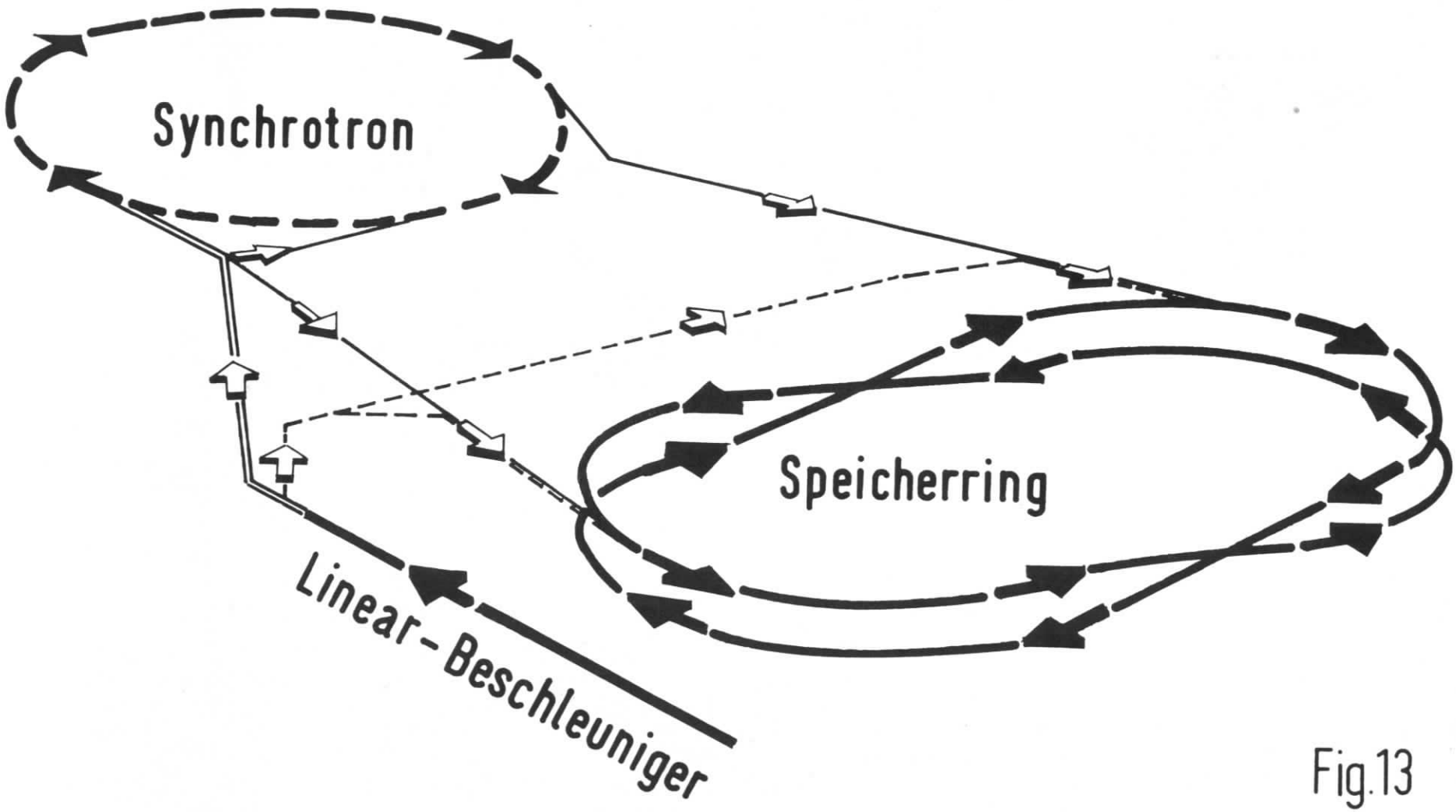

Fig.13

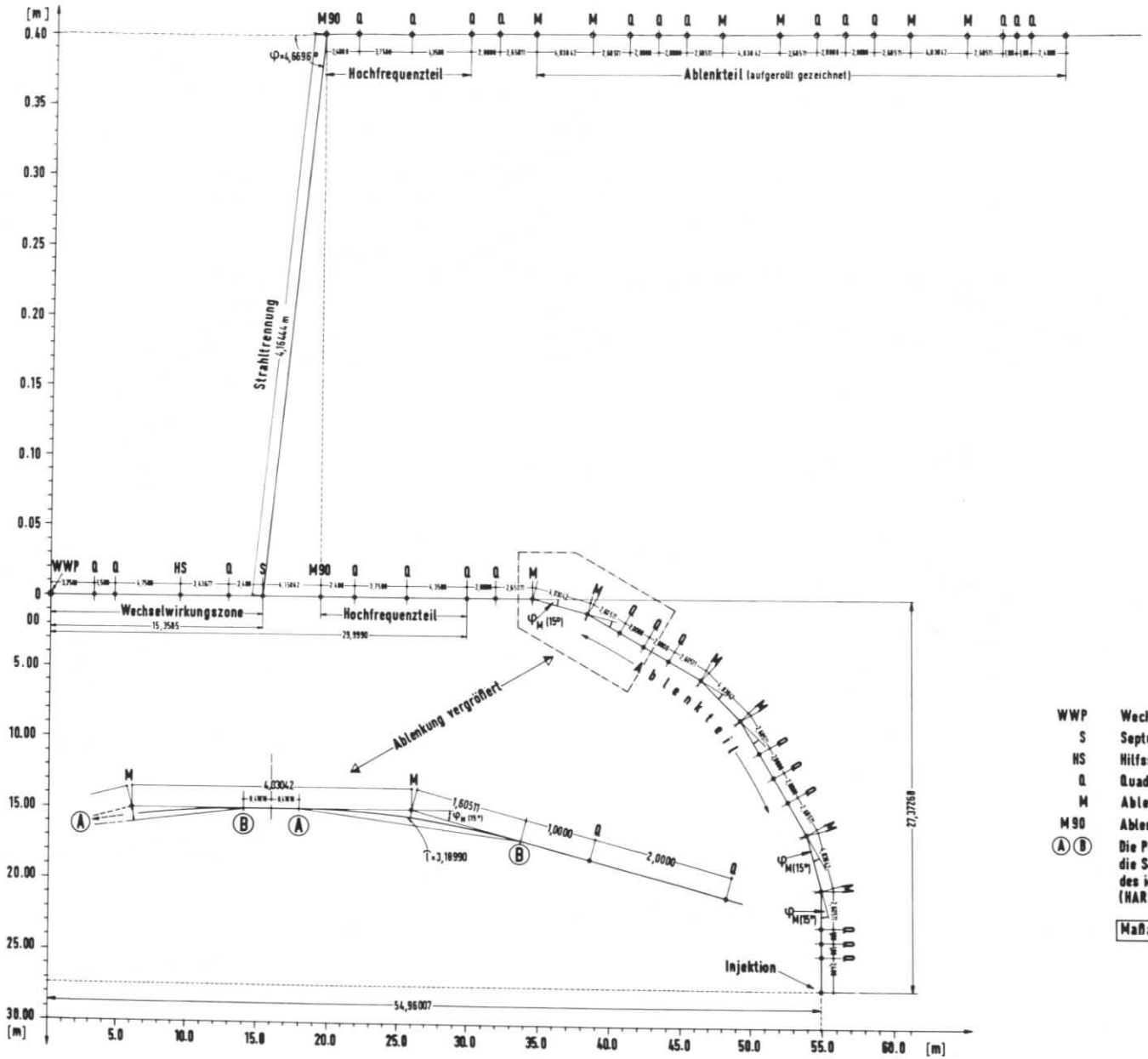

WWP	Wechselwirkungspunkt
S	Septum - Magnet
HS	Hilfsseptum - Magnet
Q	Quadrupol - Magnet
M	Ablenkmagnet
M 90	Ablenkmagnet vertikal
(A) (B)	Die Punkte (A) (B) bezeichnen die Sollbahn am Anfang und Ende des idealisierten Ablenkmagneten (HARD EDGE MODELL)

Maßangaben in Meter

Fig.14

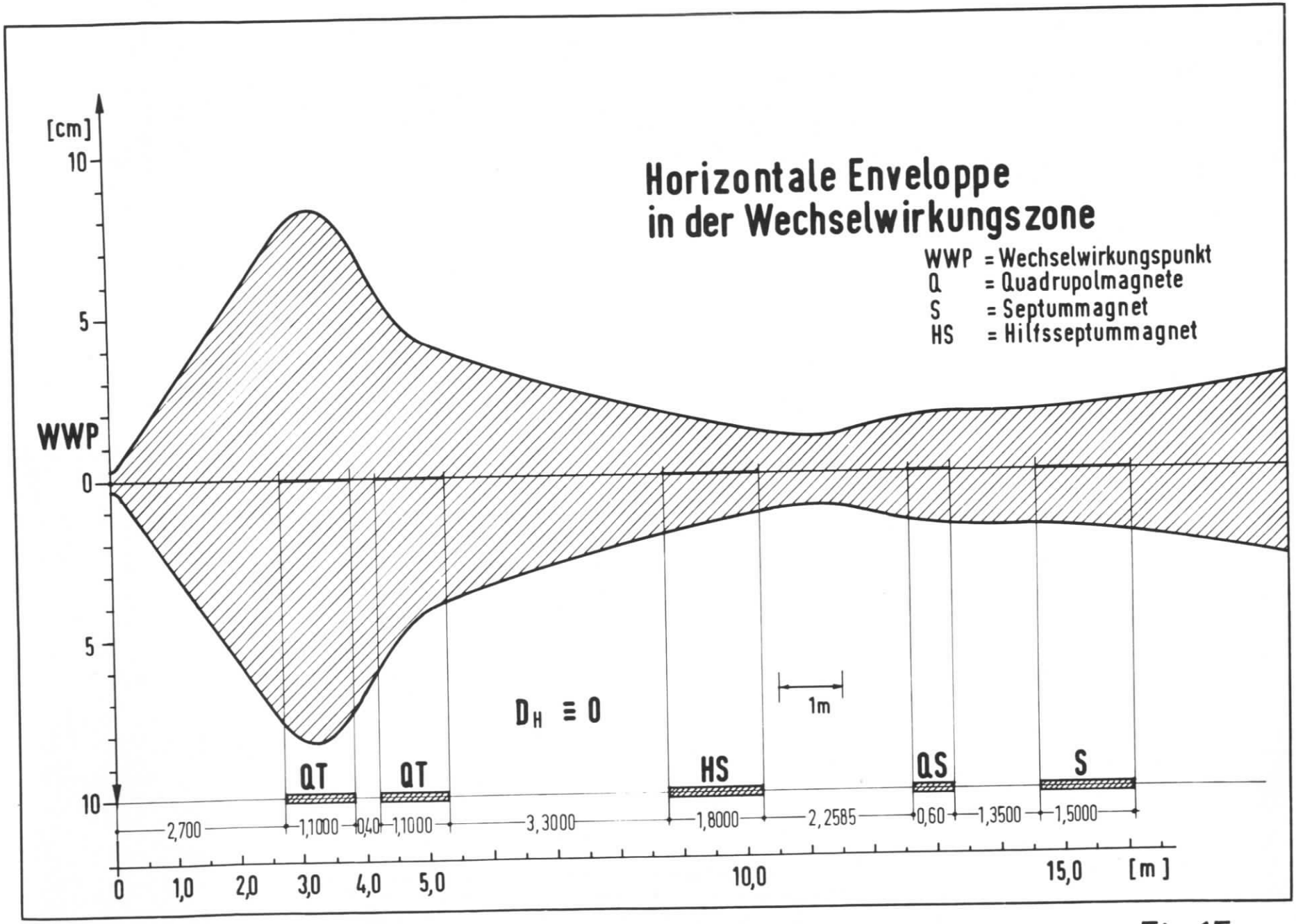
Horizontale Enveloppe
in der Wechselwirkungszone
WWP = Wechselwirkungspunkt
Q = Quadrupolmagnete
S = Septummagnet
HS = Hilfsseptummagnet
[cm]
10
5
WWP
0
5
10
$D_H \equiv 0$
1m
QT
QT
HS
QS
S
2,700
1,1000
0,40
1,1000
3,3000
1,8000
2,2585
0,60
1,3500
1,5000
0
1,0
2,0
3,0
4,0
5,0
10,0
15,0
[m]

Fig. 15